

Characterization, *in situ* electrical conductivity and thermal behavior of immobilized PEG on MCM-41

Bahaa M Abu-Zied^{1,2}, Mahmoud A. Hussein^{1,*}, Abdullah M. Asiri^{1,2}

¹ Chemistry Department, Faculty of Science, King Abdulaziz University, P.O. Box 80203, Jeddah 21589, Kingdom of Saudi Arabia

² Center of Excellence for Advanced Materials Research (CEAMR), King Abdulaziz University, P.O. Box 80203, Jeddah 21589, Kingdom of Saudi Arabia

*E-mail: maabdo@kau.edu.sa, mahusseini74@yahoo.com

Received: 11 March 2015 / Accepted: 15 April 2015 / Published: 28 April 2015

Polyethylene glycol (PEG) displayed an amazing properties when mixed with other polymers or inorganic materials. Polymers of different types (organic, inorganic or hybrid) and a variety of inorganic materials have been blended and showed interesting properties. So that, a new experimental design of PEG / MCM-41 composites has been prepared using different loading from PEG. MCM-41 as one of the most important mesoporous material has been used as support material. The preparation process for the new composites has been carried out using a simple dissolution method. Freshly prepared MCM-41 has been investigated by simple characterisation tools. The obtained structure of the new composites was promoted by various characterization techniques. which including: Fourier transform infrared spectroscopy (FT-IR), X-ray diffraction (XRD), field-emission scanning electron microscopy (FE-SEM), and thermal analyses have been used as characterization tools. Moreover, the electrical properties were measured using electrical conductivity measurements. SEM images showed nearly the same globular grain in both cases for pure MCM-41 and PEG / MCM-41_(10%) composite. Whereas PEG / MCM-41_(30%) composite showed different feature. The increasing the PEG percentage till 20 % was accompanied by a continuous decrease of the WL %.

Keywords: MCM-41, PEG, Thermal behavior, In situ electrical conductivity, Morphological properties

1. INTRODUCTION

In the last few decades, composites and nanocomposite materials have received world-wide attention in a variety of fields with a special attention to the material science. There are different types of composites or nanocomposites according to the type of composite components. One of the most important types is organic polymers based inorganic materials especially in the nano size. This type of

nanocomposite materials should have superior performance in different fields of applications with a special attention to the industrial part. Such superior performance can be appeared according to its ability to be permeable and selective for gas/liquid separation, mechanical toughness for engineering resins, and photoconductivity for electronics [1-3]. This performance of course was arrived due to the great compatibility that had been occurred between the nanoparticles as inorganic nanofiller and the polymer as a matrix in the form of new nano composite materials [4]. So many example of organic polymers that have been used as matrices to form nanocomposites with different nanoparticles such as titania, silica, carbon nanotubes, zirconia, and graphene [5 - 10]. On the other hand, much more interest has been given to the chemistry of Polyethylene glycol (PEG) and its derivatives. PEG is considered as one of the most important polymers due to it has exhibited interesting behaviors and properties such as it is commercial, non expensive, non-toxic and non-corrosive polymer. Moreover, PEG has low vapor pressure, congruently melting, high latent heat capacity, no change in its volume through solid–liquid phase convert, high chemical and thermal stability whatever the useful time is long and no super cooling [11, 12], relatively its high energy storage density, chemical stability, suitable melting point, larger heat of fusion, innocuity, low-cost and suitable phase change temperature [13]. These properties have been also arrived even when it is mingled with inorganic bearer or other polymers or when forming new composite materials. Moreover, PEG is considered as a promising phase change materials for thermal energy storage and temperature control. Among all of these properties we found that the only type of PEG that has been used as a phase change heat storage medium is low molecular-weight PEG. Of course this PEG has no ability to be stored in conventional storage tanks as it can be considered as classical solid–solid phase change substances. This type of substances and in order to prevent its leakage in the melting state, it should be packaged in special sealed tanks or containers. Furthermore, PEG has the ability be attached directly into porous materials which is considered as one of the most important property for this polymer. There is another type of PEG which is related to the solid–liquid phase change materials needs also a special treatment while restored or packaging to prevent the leakage of phase change materials during its phase transition process (solid–liquid). In the open literature there is a lack of information regarding PEG/MCM-41 composite materials.

Accordingly, the idea of this paper seeks to obtain new nanocomposite materials with several property medications by adding different ratios of the polymeric PEG to MCM-41 mesoporous materials. Several tools will be employed to check the properties of the will obtained nanocomposite. These include Fourier transform infrared spectroscopy (FT-IR), X-ray diffraction (XRD), thermal analyses (TGA, DTG and DTA), and field emission scanning electron microscopy (FE-SEM). A special attention will be given to the electrical conductivity measurements.

2. EXPERIMENTAL

2.1. Solvents and reagents

Polyethylene glycol (PEG) was obtained from Aldrich and used without any other purgation. The PEG average molecular weights is 6000. Cetyl-trimethylammonium bromide (CTAB) obtained

from Aldrich and used without purification. Tetraethyl orthosilicate (TEOS) obtained from Merck. Ethyl alcohol (> 98 %) and ammonia (28 wt. %) obtained from Prolabo. Analytical grade of ethyl acetate was also purchased from Merck Chemical Co., and used as it is without more drying or purification. Ethyl acetate was used as solvent for the preparation of these composites. Other reagents were of high purity and were further purified according to the previously reported procedure in the literature [14].

2.2. Mesoporous MCM-41 preparation

Well known mesoporous MCM-41 was prepared as reported in our previous study [15] and according to the procedure that reported by Grün et al. [16] as the following: 13.5 g of ammonia solution (28 wt. %) and 60 g of absolute ethanol were mixed together and poured into the pre-prepared surfactant solution (2.5 g of Cetyl trimethylammonium bromide (CTAB) dissolved in 50 g of distilled water). The total solution was stirred for 15 min with a constant steering rate (500 rpm), after that, 4.7 g of Tetraethyl orthosilicate (TEOS) was added at one portion leading to gel formation. Further stirring for 2hrs, the gel was aged for another 2hrs at room temperature, then filtered and washed with 300 ml of distilled water. After drying overnight at 90 °C, the sample was heated to 550 °C in air flow and kept at that temperature for 2 hrs, to remove the template then cooled to room temperature.

2.2. Preparation of PEG / MCM-41 new composite

A new experimental design of PEG / MCM-41 composites was prepared using simple dissolution method as the following: The desired composites were intended by mixing 1 g of freshly prepared and dried MCM-41 with different loading from PEG (5, 10, 15, 20 and 30%) weight by weight in about 20 mL of ethyl acetate. The reaction mixture was stirring using magnetic stirrer at the speed of 600 rpm and at nearly 60 °C for 8 - 10 hrs. This was followed by solvent evaporation in Petri dishes for at least 24 hrs at room temperature and dried under vacuum (5 and 10 Torr) for 4 - 6 hrs.

2.3. Identification and characterization techniques

Fourier transform infrared spectroscopy (FT-IR): FT-IR spectra were examined by using KBr disc technique in the wavenumber range 4000–400 cm^{-1} using Thermo-Nicolet-6700 FT-IR spectrophotometer. X-ray diffraction (XRD): Powder X-ray diffractograms were determined in the 2θ range from 4 to 70° with the aid of Philips diffractometer (type PW 103/00) using the Ni-filtered $\text{CuK}\alpha$ radiation. Scanning electron microscopy (SEM): The morphological features of the new materials were analyzed by field-emission scanning electron microscope (FE-SEM) on a JEOL model JSM-7600F microscope using EDX mode. Thermal analyses: The simultaneous TGA and DTA curves were recorded with the aid of Shimadzu DT-60 instrument apparatus. Electrical conductivity: DC electrical conductivity measurements were carried out using a Pyrex glass conductivity cell operated till 500 °C.

The resistance measurements were carried out using a Keithley 610C solid-state electrometer. In each run 500 mg of the sample were placed between two electrodes (1.0 cm diameter) and pressed by the upper electrode in order to ensure a good contact between the particles. The temperature was controlled with a WEMA temperature controller.

3. RESULTS AND DISCUSSION

PEG is considered as one of the most important polymers due to it has exhibited interesting behaviors and properties such as it is commercial, non expensive, non-toxic and non-corrosive polymer. These properties have been also arrived even when it is mingled with inorganic bearer or other polymers or when forming new composite materials. Moreover, PEG is considered as a auspicious phase change materials for thermal energy stockpiling and temperature monitoring. So that and according to the previous talk, A new controlled design of PEG / MCM-41 composites have been prepared using simple dissolution method. Initial investigations have been concentrated on the preparation of the MCM-41 as an important mesoporous material according to the well known method reported in the literatures [15, 16] as illustrated in the experimental part. The structure of MCM-41 has been confirmed by normal characterization techniques. PEG / MCM-41 new composites of different formulations depending on variable loading from PEG (5, 10, 15, 20 and 30% wt. by wt.) over MCM-41 matrix. Various characteristics of the new composites were tested and investigated in order to characterize and check the properties of the obtained composites. The effect of inclusion of PEG on the properties of mesoporous MCM-41 matrix was . A special attention was given to study in details the thermal behavior and the electrical properties using TGA thermograms and electrical conductivity measurements respectively.

3.1. Composite characterizations

The structure of the desired composites was confirmed using different characterization techniques including: FT-IR, X-ray diffraction and field emission scanning electron microscopy. FT-IR analyses are found to be an important technique and worthy instrument for the recognition of silica-supported layer silicates in different forms [17, 18] and PEG as well [19, 20]. So that, FT-IR spectroscopy gives us clear information about the bonding interactions between PEG and its matrix MCM-41 mesoporous material in the form of PEG / MCM-41_(5-30%) composites. The FT-IR spectroscopic analysis for all the samples is scanned from 4000 to 400 cm^{-1} . The FT-IR results are indicating that the PEG is combined with MCM-41 matrix in physical way. Fig. 1(a) shows the FT-IR spectra for pure MCM-41 and PEG, while Fig. 1(b) shows the FT-IR spectra for PEG / MCM-41_(5-30%) composites. The FT-IR spectra of the desired PEG / MCM-41_(5-30%) composites detect the peaks associated with neat MCM-41 and PEG peaks. It can be clarified from the data given in Fig. 1(a) for PEG and Fig. 1(b) for the new composites that, the presence of characteristic absorption bands at around 1140, 1092, and 1058 cm^{-1} with a maximum at around 1095 cm^{-1} which may be attributed to the strong triplet absorption band of the C–O–C stretching vibration. Another characteristic broad band

is observed at around $3370 - 3445 \text{ cm}^{-1}$ that attributed to the stretching vibration of hydroxyl groups. Furthermore, absorption bands at around 2885 , 963 , and 844 cm^{-1} are clearly observed. The presence of those bands are related to the stretching trembling of the $-\text{CH}_2$ functional group and to the crystal band of PEG and $\text{C}-\text{C}-\text{O}$ bonds [21, 22]. It is easily to mention all of these adsorption peaks in the spectra of the new composites as shown in Fig. 1(b).

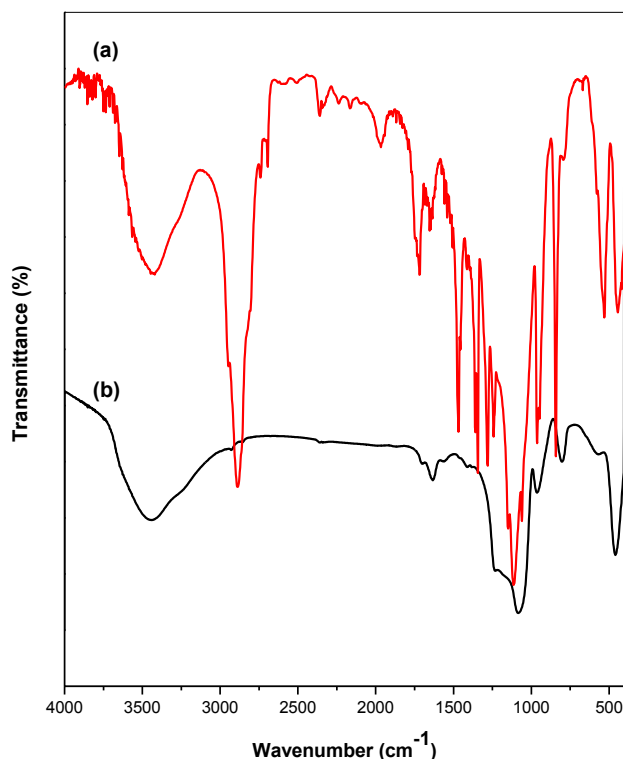


Figure 1a. FT-IR spectra of the for pure MCM-41 (a) and pure PEG (b).

On the other hand, the characteristic absorption bands for MCM-41 mesoporous material are clearly observed for pure MCM-41 and PEG / MCM-41_(5-30%) composites as illustrated in Fig. 1(a,b) respectively. This include characteristic absorption bands at around 460 cm^{-1} due to $\text{O}-\text{Si}-\text{O}$ bending vibration, at around 806 cm^{-1} due to a symmetric $\text{mSi}-\text{O}$ band and at around 1084 cm^{-1} due to an asymmetric one [23]. The shoulder around at around 1192 cm^{-1} is attributed to an outer connection mode of the SiO_4 tetrahedral, which can be found on the high-frequency side of the principal asymmetric $\text{Si}-\text{O}$ stretch [24, 25]. In addition to the previous vibrations bands, a small mOH mode vibrating band is observed at around 3441 cm^{-1} which may be due to separated final SiOH groups on the MCM-41 outer shallow with flagging acidic character, possibly with contributions from single and geminal SiOH groups as well [26 - 28]. Another peak at nearly 1633 cm^{-1} which is due to characteristic bending vibration that coming from adsorbed water. All of the previous characteristic bands are observed for our PEG / MCM-41_(5-30%) composites. Finally, it is clearly from FT-IR data to observe

that, as the amount of PEG increases (5-30%) its corresponding characteristics absorption bands increase. Mean while, the characteristics MCM41 absorption bands decrease within the same order.

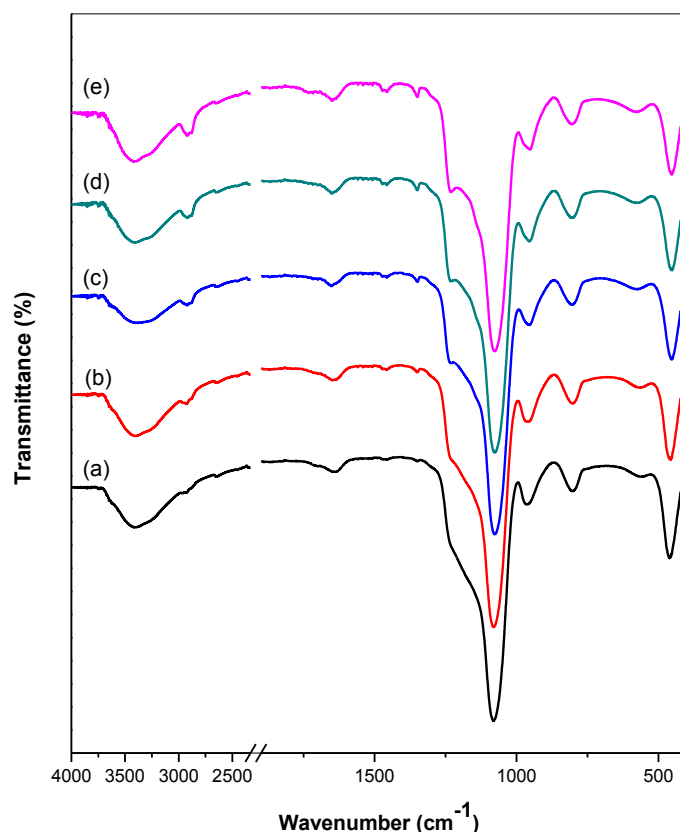


Figure 1b. FT-IR spectra of the for for PEG / MCM-41_(5%) (a), PEG / MCM-41_(10%) (b), PEG / MCM-41_(15%) (c), PEG / MCM-41_(20%) (d), PEG / MCM-41_(30%) (e) composites.

The XRD diffraction patterns for PEG / MCM-41_(5-30%) composites, over the range of $2\theta = 5^\circ - 70^\circ$, are shown in Fig. 2. Both pure PEG and mesoporous MCM-41 material have the ability to merge to each other by physical meaning through the composite consistence. It is well known that, the low angel X-ray diffraction pattern of ordered mesoporous MCM-41 exhibits a strong peak in the range of $2\theta = 1.8 - 2.8^\circ$ and the weak peaks in the range of $2\theta = 3.5 - 4.8^\circ$ and $2\theta = 5.6 - 6.7^\circ$ [20, 29-31]. Furthermore, the pure PEG displays reflection beaks in the range of $2\theta = 14.65 - 45.15^\circ$ and exactly showed at $2\theta = 14.65^\circ, 15.08^\circ, 19.16^\circ, 23.25^\circ, 26.19^\circ, 26.92^\circ, 27.85^\circ, 30.90^\circ, 32.67^\circ, 36.13^\circ, 39.69^\circ, 42.94^\circ,$ and 45.15° [32, 33]. A close inspection of Fig. 2 reveals that, the presence of characteristic amorphous like nature of silica in all PEG / MCM-41_(5-30%) compositions, which is commonly achieved for MCM-41 materials in the range of $2\theta = 14 - 35^\circ$ [34, 35]. Whereas, the pattern for the PEG / MCM-41_(5%), PEG / MCM-41_(10%), PEG / MCM-41_(15%) and even PEG / MCM-41_(20%) materials does not show any extra peaks in the hole range. However, for the PEG / MCM-41_(30%) composite, a few and small reflection beaks can be detected around positions of the major distinctive lines for PEG at $28.55^\circ, 47.47^\circ,$ and 56.33° , respectively. These are in correspondence with

that observed for pure PEG. There is no further peaks that may be attributed to the existence of impurities or other stages were adjusted. It is also notice that, the increase of the PEG content is accompanied by a gradual decrease for the reflection that related to amorphous halo beak of silica which obtained for MCM-41 mesoporous material.

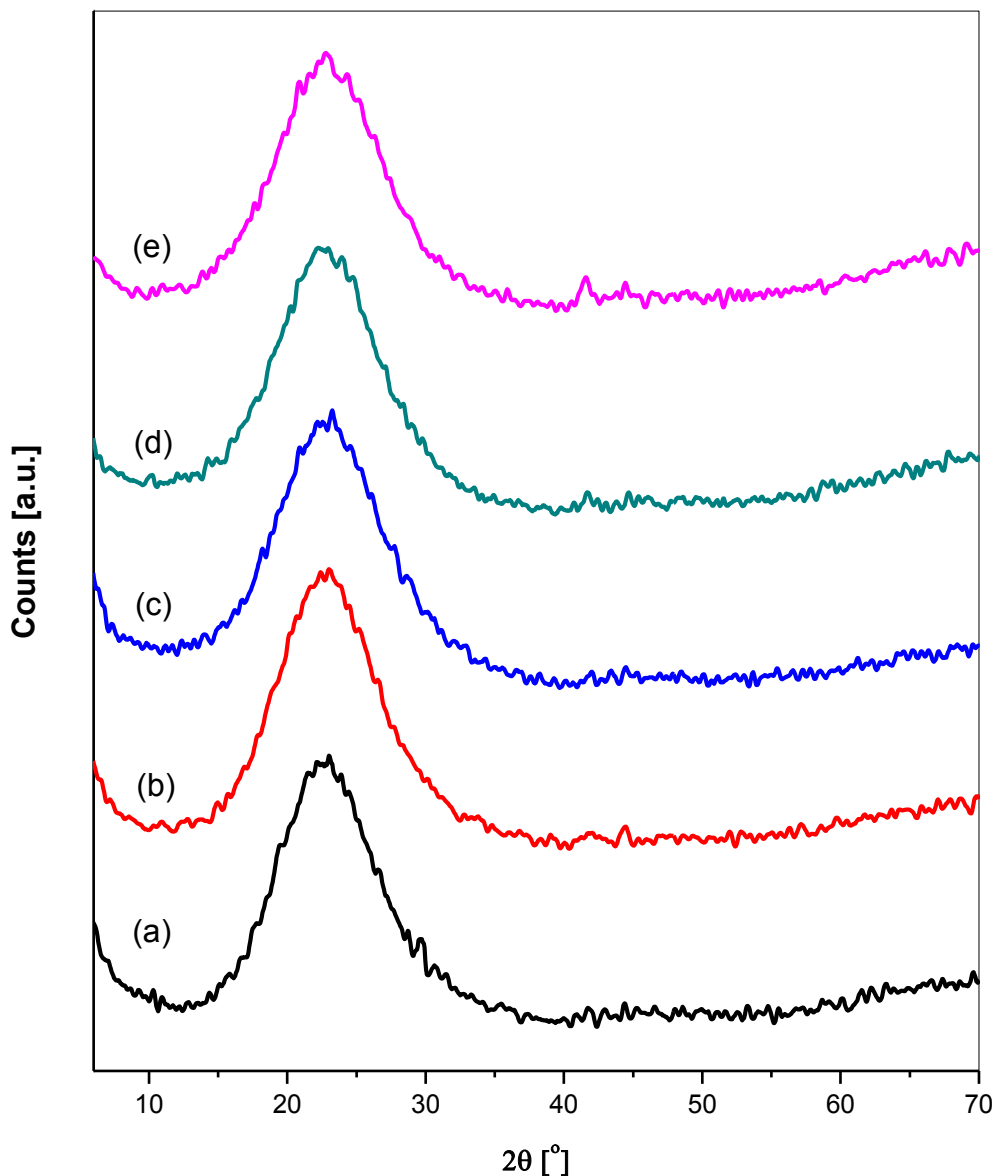


Figure 2. Wide-angle XRD diffractograms obtained for PEG / MCM-41_(5%) (a), PEG / MCM-41_(10%) (b), PEG / MCM-41_(15%) (c), PEG / MCM-41_(20%) (d), PEG / MCM-41_(30%) (e) composites.

The morphological photographs of pure MCM-41 and PEG / MCM-41_(10, 30%) composites have been fully considered by FE-SEM micrographs as shown in Fig. 3. The measured samples having similar globular agglomerations with a little changes in case of PEG / MCM-41_(30%). Moreover, we can observe the presence of infrequent graves, are distributed between them. These graves appear to

have no specific size or modality. Fig. 3(a,b) depict the SEM micrographs of pure MCM-41. The figures show that the surface of the pure mesoporous MCM-41 material appears as accumulative globular and semi-globular particles having an average diameter of 250–500 nm with magnifications of $x = 37,000$ and $50,000$.

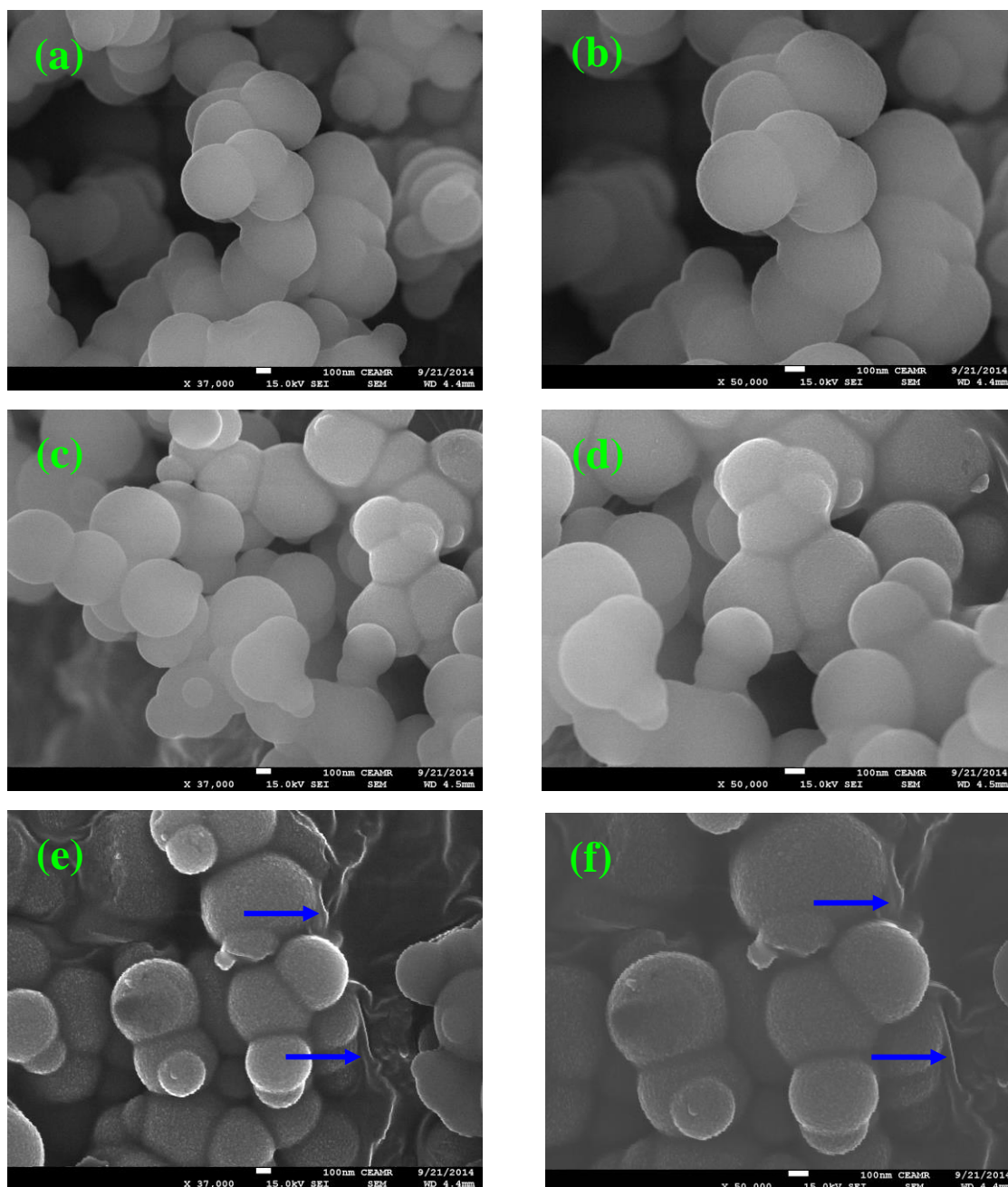


Figure 3. FE-SEM micrographs for neat MCM-41 (a,b), PEG / MCM-41_(10%) (c,d), and PEG / MCM-41_(30%) (e,f).

Despite being a composite in nature, almost the same shape and size of the globular grains are observed from the SEM images under the same magnifications ($x = 37,000$ and $50,000$) for PEG / MCM-41_(10%) as shown in Fig. 3(c,d) . This observation can be explained that the loaded ratio of PEG filler (10%) have been completely entered into a pipeline of MCM-41 matrix and hence it is completely disappeared. By another words we can say, MCM-41 tube lines are filled with PEG during the composite formation. On the other hand, Fig. 3(e,f) (magnifications $x = 37,000$ and $50,000$) show the morphological photographs for PEG / MCM-41_(30%) composite. The images show that, PEG start to appear as a clear evidence for the composite consistence. The images also show that, there is great coalescence between the PEG as a filler and the MCM-41 as a matrix, which is very important to conduct a tight interfacial adherence. In order to understand the observed changes in textural data for this composition. We can say that, the globular grains of MCM-41 have start to be covered by the excess of PEG after complete filling of the pipeline of MCM-41 tubes.

3.2. Thermal behavior:

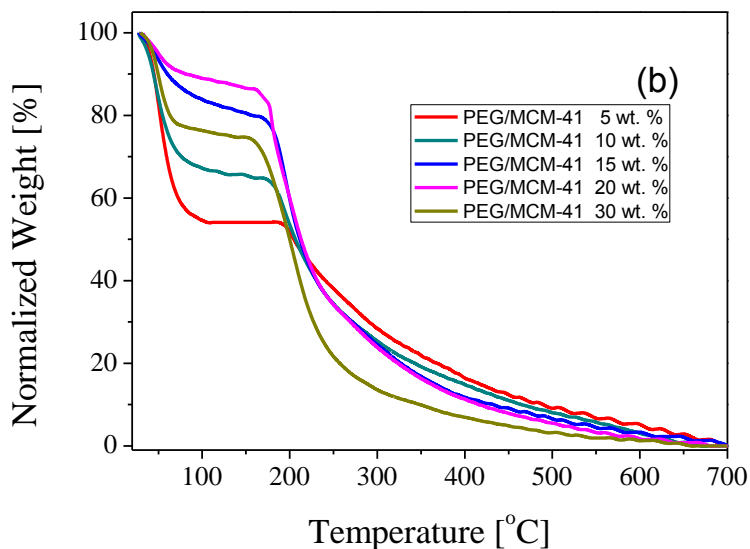
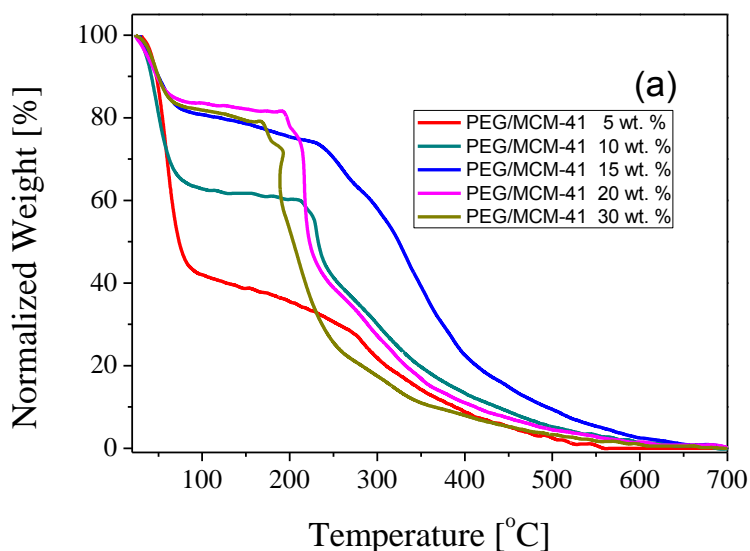


Figure 4. TGA curves of the various MCM-41/PEG composites obtained under air (a) and N₂ (b).

The thermal behavior of the various PEG/MCM-41 composites were investigated using TGA analysis. Fig. 4(a), and (b) shows the normalized weight loss (NWL) curves acquired for the composites under investigation in air and nitrogen flows, respectively. Generally, the NWL is defined mathematically as follows; $NWL = 100 \times [(w - w_{MCM-41}) / (w_0 - w_{MCM-41})]$, where w , w_{MCM-41} , and w_0 represent the weight of the composite at temperature T , the weight of MCM-41 loaded, and the initial weight of composite, respectively. An early weight loss (WL), below 160 °C, can be observed for all the samples. This WL can be specified to the elimination of adsorbed water molecules [15, 19, 20, 36]. Table 1 lists the WL of the various samples at 150 °C in both atmospheres. It is obvious that increasing the PEG percentage till 20 % is accompanied by a continuous decrease of the WL %. Meanwhile, the observed WL values in N₂ flow is lower than the relevance ones in air. This finding suggests that increasing the MCM-41 content, i.e. at lower PEG percentage, enhances the hydrophilicity of the obtained composite.

Table 1. WL of the various composites at 150 °C.

Sample	WL in air [%]	WL in N ₂ [%]
PEG/MCM-41-5	61.4	45.9
PEG/MCM-41-10	38.5	34.5
PEG/MCM-41-15	21.5	19.4
PEG/MCM-41-20	17.9	13.4
PEG/MCM-41-30	20.3	25.5

Fig. 4(a) indicates that the polymer starts to decompose throughout three consecutive steps in air, which start at temperatures 160 °C. In N₂ flow Fig. 4(b), it appears that the first two decomposition steps are emerged in a single one. Table 2 shows the T₅₀ and T₈₀ values (the temperatures of 50 % and 80% weight loss, respectively). Higher T₅₀ and T₈₀ values reflects higher thermal behavior of the polymer. From the combination of the data presented in Fig. 4 and Table 2 the following two points could be abstracted: (i) the T₅₀ value is shifted towards higher temperatures on increasing the PEG content till PEG percentage of 15 and 20 % in air and nitrogen, respectively, at higher PEG contents it is shifted towards lower temperatures, and (ii) the observed temperatures shift is much more pronounced in air than in nitrogen flows. In the open literature, there are various reports concerning the influence of MCM-41 on the thermal stability of polymers matrices. For instance, Marcilla et al. demonstrated that the addition of MCM-41 to polyethylene [37], polypropylene [38] polystyrene and ethylene-e-vinyl acetate copolymer [39-41] induces a remarkable decrease in the temperature of the maximum decomposition of these polymers. In agreement, a reduction in the temperatures required to decompose polypropylene was reported during the addition of Al-MCM-41 [42] and Al-MCM-48 [43]. In the former reports, the observed lowering in the temperature of maximum decomposition of the

polymers was ascribed to the catalytic effect of the MCM-41 acid sites. The obtained results are in correspondence with these literature data by confirming that the lower PEG percentage the sample, i.e. the higher MCM-41 content, the lower is the decomposition temperature of the composite. However, we have observed a shift of the composite-decomposition temperature for the sample with PEG percentage of 30 % in nitrogen and the two samples having 20 and 30 % PEG in air. This, in turn, suggests a dependence of the locations of the polymer molecules on its content. In other words, at lower PEG content in the composite (till around 20 %) the polymer molecules could be immobilized inside the MCM-41 channels and at higher contents the polymer starts to be located at outer the MCM-41 channels. The last WL step shown in Fig. 4 proceeds with a slow rate and extends over a wide range of temperatures (300-700 °C). In agreement with our previous studies [15,19,20], this step could be attributed to the slow removal of the non-volatile carbonaceous residues, which were formed during the main degradation process.

Table 2. TGA data of PEG/MCM-41 composites in air and nitrogen atmospheres.

Sample	Air flow		N ₂ flow	
	T ₅₀ [°C]	T ₈₀ [°C]	T ₅₀ [°C]	T ₈₀ [°C]
PEG/MCM-41-5	74	307.9	205.6	366.7
PEG/MCM-41-10	233	347.1	207.6	345.4
PEG/MCM-41-15	328.4	414.1	210.9	328.1
PEG/MCM-41-20	222.6	232.7	212.7	321.7
PEG/MCM-41-30	204.6	282.2	200.0	256.1

Based on the above results, a schematic illustration for the formation of PEG/MCM-41 composites is shown in Fig. 5. The calcined MCM-41 mesoporous material possess the well-defined pore structure resulting from the condensation of Si–OH groups. When the PEG is loaded into the MCM-41 channels it reacts with the various Si–OH groups located inside the channels via hydrogen bonds formation. From the TGA results, it is plausible to suggest that at low PEG content the PEG molecules are immobilized mostly via adsorption on the inner pore wall of the MCM-41. Increasing the PEG loading till approximately 20 % is accompanied by a complete filling of the MCM-41 channels. Upon further increase of the PEG loading to 30 % the added PEG molecules will be coated on the outer surface of the MCM-41 material.

3.3. *In situ* electrical conductivity

In situ electrical conductivity is supposed to be as the most motivating tool that gives insight about the variation of the electrical properties of the solid material during its heating [15,19,44]. Fig. 6 shows the temperature dependence of $\log \sigma$ obtained for neat MCM-41 and PEG/MCM-41 composites with PEG percentage of 5 and 30 %.

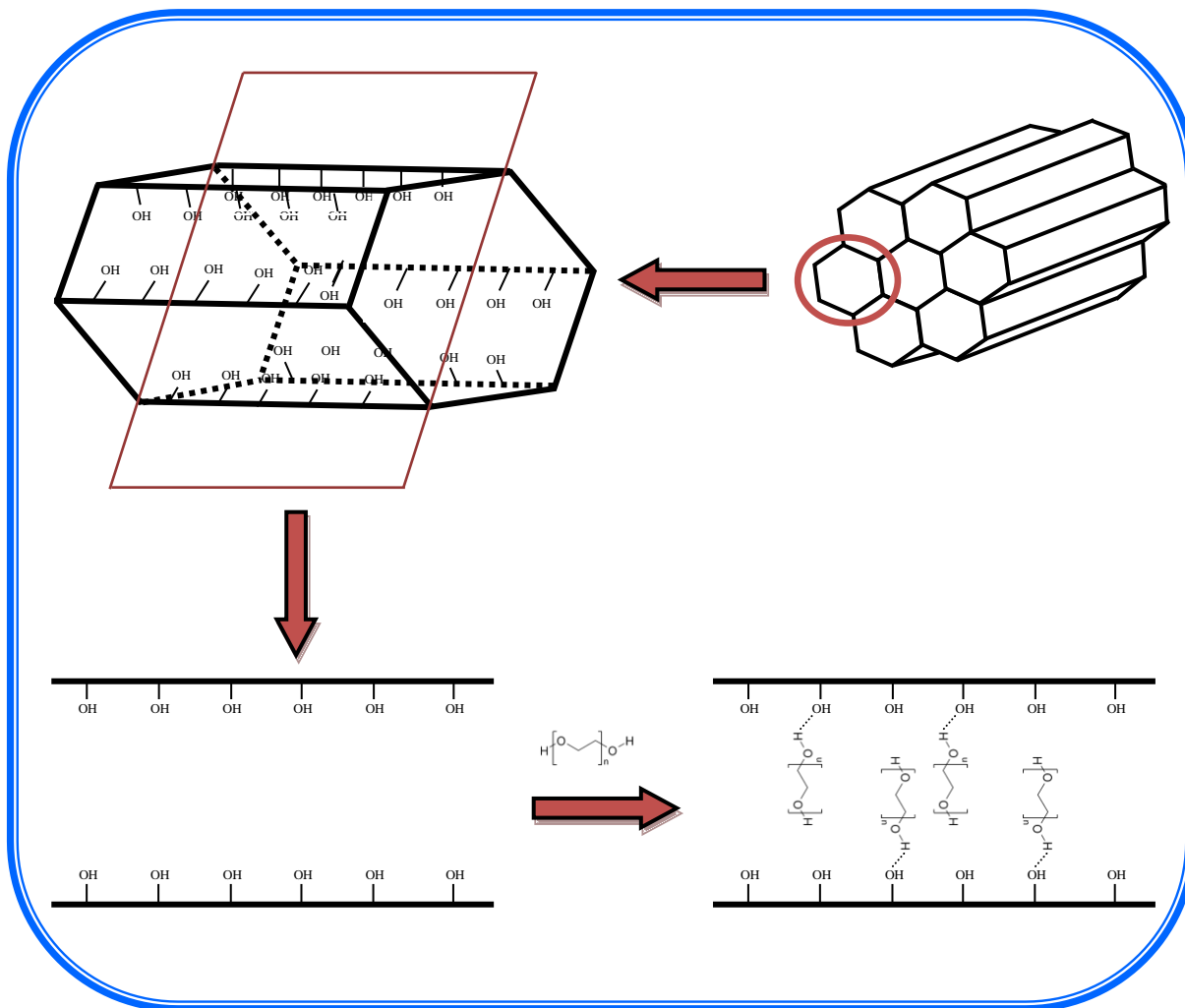


Figure 5. Schematic illustration of the interaction of PEG with MCM-41 material.

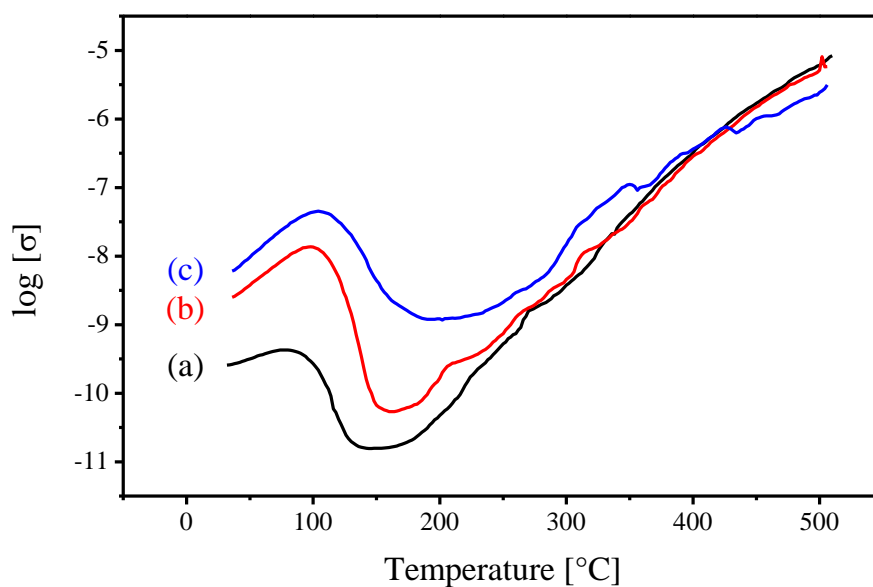


Figure 6. Plots of $\ln \sigma$ vs. temperature for neat MCM-41 (a), PEG/MCM-41 5 wt. % (b) and PEG/MCM-41 30 wt. % (c) composite.

From the inspection of Fig. 6 it appears that at ambient temperature, the conductivity values of the composites are higher than the neat MCM-41. Meanwhile, the conductivity increases with increasing the PEG content. This observation, in turn, suggest that the mobility of the charge carriers of the composites is higher than the neat MCM-41 material and this mobility increases with increasing the PEG loading. In this context, it was reported that the conductivity in the zeolite based materials is related to the ability of the exchangeable cations, M^{n+} and H^+ ions, to migrate along the tube lines and cavities of the zeolite framework via an ion-hopping mechanism [45]. The cations motion is spotted by the electrostatic attraction occurred between them and the negatively charged framework of the zeolite material together with steric effects caused by the size of these cations [45,46]. In combination with the suggest scheme for the composite formation, it seems that the H^+ ions of the Si-OH groups movement is facilitated throughout the formation of hydrogen bonds with the loaded PEG molecules.

The obtained plots in Fig. 6 can be divided into three regions. The first one extends from ambient to 80, 98 and 106 °C for the neat MCM-41, PEG/MCM-41 5% and PEG/MCM-41 30, respectively. In that region, the conductivity increases continuously with the temperature rise, which can be correlated with the removal of adsorbed water molecules from the solids. This increase is parallel to that observed in the literature for ZSM-5/PEG [19] and MCM-41/PEG [15] composites. In the second region, which extends to 155-190 °C, one can observe a decrease in the conductivity. This can be correlated with the completion of solids dehydration. Meanwhile, the conductivity values of the three samples still showing the same order, i.e. PEG/MCM-41 30% > PEG/MCM-41 5% > MCM-41. In the third region, which extends till 500 °C (the temperature limit of our conductivity cell), a continuous conductivity increase can be observed. This behavior can be correlated with the decomposition of the PEG molecules together with the positive influence of rising the temperature, which enhances the movement of the charge carriers. In this region the composite materials are still showing higher conductivity than the neat MCM-41 till around 420 °C; a temperature after which a lower conductivity is exhibited by the PEG/MCM-41 30 % sample. Bearing in mind the fact that the formation of non-volatile carbonaceous residues at the temperature range of 400-700 °C for the different composites (Fig. 4), it is reasonable to suggest that these residues plays significant role in hindering the movement of the charge carriers. Thus, the observed lower conductivity values for the PEG/MCM-41 30 % sample than the neat MCM-41 at temperatures > 420 °C could be related to the presence of these non-volatile carbonaceous residues that hinder the movement of the charge carriers. Similar argument was used to interpret the conductivity trend of the calcined ZSM-5/PEG composites [19].

4. CONCLUSIONS

New design of PEG / MCM-41 composites are prepared using simple dissolution method. PEG of different loading (5-30%) are used as filler to form the targeted composites. PEG is physically interacting with mesoporous MCM-41 material proceeding the composite. PEG content is consumed inside the tube lines of MCM-41 until PEG / MCM-41_(20%) , after that it starts to flow outside. PEG / MCM-41_(30%) shows a small reflection beaks that related to PEG have been started to be observed. This

observation is in accordance with that observed in the FE-SEM images. The observed WL values in N₂ flow is lower than the relevance ones in air. This finding suggests that increasing the MCM-41 content, i.e. at lower PEG percentage, enhances the hydrophilicity of the obtained composite. The T₅₀ value is shifted towards higher temperatures on increasing the PEG content till PEG percentage of 15 and 20 % in air and nitrogen, respectively. The observed temperatures shift is much more pronounced in air than in nitrogen flows.

ACKNOWLEDGEMENT

This work was funded by the Center of Excellence for Advanced Materials Research (CEAMR), King Abdulaziz University, Jeddah under grant no. (CEAMR-SG-6-435). The authors, therefore, acknowledge with thanks CEAMR technical and financial support.

References

1. G.W. Peng, F. Qiu, V.V. Ginzburg, D. Jasnow and A.C. Balazs, *Science*, 288 (2000) 1802.
2. T.C. Merkel, B.D. Freeman, R.J. Spontak, Z. He, I. Pinnau, P. Meakin and A.J. Hill, *Science*, 296 (2002) 519.
3. Y. Wang and N. Herron, *Science*, 273 (1996) 632.
4. J. He, Y. Shen, D. G. Evans and X. Duan, *Composites: Part A*, 37 (2006) 379.
5. D.W. McCarthy, J.E. Mark, S.J. Clarson and D.W. Schaefer, *J. Polym. Sci. Part B Polym. Phys.*, 36 (1998) 1191.
6. M. Motomatsu, T. Takahashi, H.Y. Nie, W.H. Mizutani and H. Tokumoto, *Polymer*, 38 (1997) 177.
7. G.Canché-Escamilla, S. Duarte-Aranda and M. Toledano *Materials Science and Engineering: C*, 42 (2014) 161.
8. A. Zendehnam, S. Mokhtari, S.M. Hosseini, M. Rabieyan, *Desalination*, 347 (2014) 86.
9. K. Kompany, Humayun E. Mirza, S. Hosseini, B. Pinguan-Murphy and I. Djordjevic, *Materials Letters*, 126 (2014) 165.
10. P. Zhai, Y-H. Chang, Y-T. Huang, T-Ch. Wei, H. Su and Sh-P. Feng, *Electrochimica Acta*, 132(2014) 186.
11. K. Pielichowski and K. Flejtuch, *Polymers for Advanced Technologies*, 13 (2002) 690.
12. C. Alkan, A. Sari, Uzun. and O. Amer, *Inst. of Chem. Eng. J*, 52 (2006) 3310.
13. K. Pielichowski and K. Flejtuch, *Polym. Adv. Technol.*, 13 (2002) 690.
14. D.D. Perrin, W.L.F. Armario and D.F. Perrin, *Purification of Laboratory chemicals*, 2nd ed Pergamon, New York, (1980).
15. B. M. Abu-Zied, M. A. Hussein, and A. M. Asiri, *Int. J. Electrochem. Sci.*, 10 (2015) 1372 - 1383
16. M. Grün, K. K. Unger, A. Matsumoto and K. Tsutsumi, *Micropor. Mesopor. Mater.*, 27 (1999) 207.
17. M. Kermarec, J.Y. Carriat, P. Burattin, M. Che, A. Decarreau, *J. Phys. Chem.*, 98(1994) 12008.
18. P. Burattin, M. Che, C. Louis, *J. Phys. Chem. B*, 101 (1997) 7060.
19. M. A. Hussein, B. M. Abu-Zied and A. M. Asiri, *Polymer Composites*, 35 (2014), 1160.
20. M. A. Hussein, B. M. Abu-Zied and A. M. Asiri, *Composites: Part B*, 58 (2014) 185.
21. W.L. Wang, X.X. Yang, Y.T. Fang, J. Ding, J.Y. Yan, *Applied Energy*, 86 (2009) 1479.
22. W.L. Wang, X.X. Yang, Y.T. Fang and J. Ding, *Applied Energy*, 86 (2009) 170.
23. M. Broyer, S. Valange, J.P. Bellat, O. Bertrand, G. Weber, Z. Gabelica, *Langmuir*, 18 (2002) 5083.
24. E.M. Flanigen, H. Khatami, H.A. Szymanski, in: E.M. Flanigen, L.B. Sand (Eds.), *Molecular Sieve Zeolites-I*, American Chemical Society, Washington, DC, (1974) pp. 201.

25. S.M. Holmes, V.L. Zholobenko, A. Thursfield, R.J. Plaisted, C.S. Cundy, J. Dwyer, *J. Chem. Soc., Faraday Trans.*, 94 (1998) 2025–2032.
26. A. Jentys, N.H. Pham, H. Vinek, *J. Chem. Soc., Faraday Trans.*, 92 (1996) 3287.
27. J. Chen, Q. Li, R. Xu, F. Xiao, *Angew. Chem. Int. Ed.* 34 (1995) 2694.
28. X.S. Zhao, G.Q. Lu, A.K. Whittaker, G.J. Millar, H.Y. Zhu, *J. Phys. Chem. B*, 101(1997) 6525.
29. S.G. Aspromonte, A. Sastre, A.V. Boix, M.J. Cocero and E. Alonso, *Micropor. Mesopor. Mater.*, 148 (2012) 53.
30. T. Lehmann, T. Wolff, C. Hamel, P. Veit, B. Garke and A. Seidel-Morgenstern, *Micropor. Mesopor. Mater.*, 151 (2012) 113.
31. V.N. Jayaratne, S.L.Y. Chang, X. Fang and A.L., *Micropor. Mesopor. Mater.*, 151 (2012) 466.
32. L. Zhang, J. Zhu, W. Zhou, J. Wang and Y. Wang, *Energy*, 39 (2012) 294.
33. L. Feng, J. Zheng, H. Yang, Y. Guo, W. Li and X. Li, *Sol Energy Mater Sol Cells*, 95 (2011) 644.
34. K. M. S. Khalil, *J. Coll. Interf. Sci.*, 315 (2007) 562.
35. W. Yao, Y. Chen, L. Min, H. Fang, Z. Yan, H. Wang, J. Wang, *J. Molec. Catal. A Chem.*, 246 (2006) 162.
36. A. Jomekian, S.A.A. Mansoori and N.Monirimanesh, *Desalination*, 276 (2011) 239.
37. A. Marcilla, A. Gómez, Á.N. García and M.M. Olaya. *J. Anal. Appl. Pyrol.*, 64 (2002) 85.
38. A. Marcilla, A. Gómez, J.A. Reyes-Labarta and A. Giner, *Polym. Degrad. Stabil.*, 80 (2003) 233.
39. A. Marcilla, A. Gómez and S. Menargues, *Polym Degrad Stabil*, 89 (2005) 145.
40. A. Marcilla, A. Gómez-Siurana, J.C. García Quesada and D. Berenguer, *Polym. Degrad. Stabil.*, 92 (2007) 1867.
41. A. Marcilla, A. Gómez-Siurana, S. Menargues, R. Ruiz-Femenia and J.C. García-Quesada, *J. Anal. Appl. Pyrol.*, 76 (2006) 138.
42. B. Saha, P. Chowdhury and A.K. Ghoshal, *Appl. Catal. B: Environ.*, 83 (2008) 265.
43. H.J. Park, J.-H. Yim, J.-K.Jeon, J.M. Kim, K.-S. Yoo and Y.-K. Park, *J. Phys. Chem. Solids*, 69 (2008) 1125.
44. S.A. Soliman and B.M. Abu-Zied, *Thermochim. Acta*, 491 (2009) 84.
45. G. Kelemen and G. Schön, *J. Mater. Sci.*, 27 (1992) 6036.
46. F.J. Jansen and R.A. Schoonheydt, *J. Chem. Soc. Farady Trans. 1*, 69 (1973) 1338.